

## Accepted Manuscript

A highly efficient and versatile carbon nanotube/ceramic composite filter

Hamed Parham, Steven Bates, Yongde Xia, Yanqiu Zhu

PII: S0008-6223(12)00923-2

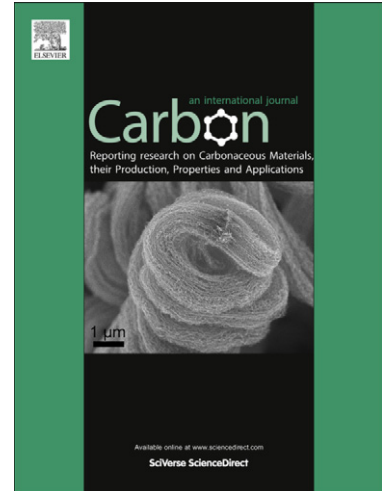
DOI: <http://dx.doi.org/10.1016/j.carbon.2012.11.032>

Reference: CARBON 7651

To appear in: *Carbon*

Received Date: 18 September 2012

Accepted Date: 14 November 2012



Please cite this article as: Parham, H., Bates, S., Xia, Y., Zhu, Y., A highly efficient and versatile carbon nanotube/ceramic composite filter, *Carbon* (2012), doi: <http://dx.doi.org/10.1016/j.carbon.2012.11.032>

This is a PDF file of an unedited manuscript that has been accepted for publication. As a service to our customers we are providing this early version of the manuscript. The manuscript will undergo copyediting, typesetting, and review of the resulting proof before it is published in its final form. Please note that during the production process errors may be discovered which could affect the content, and all legal disclaimers that apply to the journal pertain.

**A highly efficient and versatile carbon nanotube/ceramic composite filter****Hamed Parham<sup>a</sup>, Steven Bates<sup>b</sup>, Yongde Xia<sup>a</sup>, Yanqiu Zhu<sup>a,\*</sup>**<sup>a</sup> College of Engineering Mathematics & Physical Sciences, University of Exeter,<sup>b</sup> College of Life and Environmental Sciences, University of Exeter,

Exeter, Devon, EX4 4QF, UK

**Abstract**

Carbon nanotubes were grown in the open pores of a commercial porous ceramic matrix consisting of mainly Al<sub>2</sub>O<sub>3</sub> and SiO<sub>2</sub> with an average pore size of 300 μm and 500 μm, using a pre-formed nickel catalyst inside the pores and a camphor solution precursor at 780°C. The resulting composites, Ø27 mm × 10 mm discs containing about 3 wt% of carbon nanotubes, were then assessed as a filter for the removal of yeast cells and different heavy metal ions from water, and for the removal of particulates from air. The results showed that the carbon nanotube containing composite filter demonstrated a high efficiency of yeast filtration (98%), *ca.* 100% heavy metal ion removal from water and excellent particulate filtration from air. The composite filter also exhibited good reusability for these applications, owing to the excellent thermal and chemical stability of the carbon nanotubes.

**\* Corresponding author:**

Fax: +44 1392 217965. E-mail address: y.zhu@exeter.ac.uk (Y. Q. Zhu)

## 1. Introduction

Pollution is one of the major problems facing mankind today, representing a severe threat to natural resources and our health. The threat of pollutants and contaminants arises from different sources, including submicron and nanosized particles in polluted air which can cause respiratory problems [1]. In addition heavy metal ions, toxic chemicals and pathogens in contaminated water can also impact our daily life, as well as a variety of industries including pharmaceutical manufacturing and food production [2]. In particular heavy metal ions in wastewater, from metallurgical industries, mining and battery manufacturing, can accumulate in living tissues to toxic or carcinogenic levels. Stringent standards are now in place to regulate their discharge and methods have been developed for their removal from the aquatic environment [3]. However, new technologies are in constant demand for the reduction and complete removal of these harmful contaminants in order to improve the quality of life.

Nanofibres and nanotubes have emerged as a promising filtration material, and nanomaterials have received widespread interest for water and air purification. In particular carbon nanotubes (CNTs), owing to their high surface area and large aspect ratio, have received special attention focused on their excellent nanosorbent properties for filtering contaminants from water [4]. As such the ability of CNTs, embedded in membranes or supported on other structural media such as a metal or ceramic truss, has been explored for the construction of a wide range of new filters [5, 6]. In terms of the filtration of particulates from the air it has been shown that a CNT network of micro-or meso-pores [4] or CNTs grown on micromachined Si/SiO<sub>2</sub> [7], stainless steel [8] or glass fibres [9] can show good filtration efficiencies for various particle sizes. In addition CNT filters developed on glass fibres [9], through macro architecture [10] or on microporous membranes [11, 12] has been shown to be efficient in the removal of bacterial and viral pathogens from water, and even

result in the inactivation of the pathogen. Finally the adsorption capability of CNTs for a wide range of metal ions, including  $\text{Cu}^{2+}$ ,  $\text{Pb}^{2+}$ ,  $\text{Cd}^{2+}$  [3],  $\text{Zn}^{2+}$ ,  $\text{Mn}^{2+}$ ,  $\text{Co}^{2+}$  [13],  $\text{Ni}^{2+}$  [14],  $\text{Cr}^{2+}$  [15],  $\text{Hg}^{2+}$  [16] and  $\text{U}^{6+}$  [17] has been investigated and these typically show different orders of affinity depending on the functionalization and synthesis procedures employed. This would suggest that heavy metal ion adsorption by CNTs is a chemisorption process, resulting from chemical interactions involving valence (bond) forces and the sharing or exchange of electrons [18]. In addition CNTs display the added benefit that the adsorbed metal ions can be desorbed and thus CNTs can be reused [19]. The immediate technological challenge now is how to convert the excellent adsorption behaviour of loose CNT powder into a cost effective and viable filter for specific applications, akin to the breakthroughs made in using CNTs to filter oil [10].

In this report, we demonstrate a simple approach to construct highly efficient and versatile CNT composite filters by direct growth of CNTs on a porous ceramic matrix. The performance of these new filters was assessed for the removal of yeast and heavy metal ions from water, and particulates from the air. Further development of these filters may lead towards their practical application.

## 2. Experimental

### 2.1 Synthesis of composite

Camphor ( $\text{C}_{10}\text{H}_{16}\text{O}$ , 96%, Sigma-Aldrich) was used as a carbon source with nickel (II) nitrate hexahydrate crystals ( $\text{Ni}(\text{NO}_3)_2 \cdot 6\text{H}_2\text{O}$ , Sigma-Aldrich) as the catalyst precursor. Porous ceramics of pore size 300 and 500  $\mu\text{m}$ , (o.d.  $27 \times 10$  mm, Dynamic-Ceramic Ltd, UK), with a chemical composition of 81%  $\text{Al}_2\text{O}_3$ , 14%  $\text{SiO}_2$ , 2.5%  $\text{K}_2\text{O}$ , 2.5%  $\text{Na}_2\text{O}$  and 2.5% other minute oxides ( $\text{TiO}_2$ ,  $\text{Fe}_2\text{O}_3$ ,  $\text{MgO}$ ,  $\text{CaO}$  and  $\text{Cr}_2\text{O}_3$ ), were used as the matrix to support CNT growth. First, 1 wt. %  $\text{Ni}(\text{NO}_3)_2 \cdot 6\text{H}_2\text{O}$  was dissolved in acetone and the porous ceramic discs were dipped in the solution in order to introduce the catalyst precursor onto the

surface of the pores. The acetone was then evaporated before placing the ceramic matrix containing  $\text{Ni}(\text{NO}_3)_2 \cdot 6\text{H}_2\text{O}$  in a quartz working tube (i.d. 27 mm) and moving to a horizontal tube furnace. Air was then flushed out of the quartz tube using Ar before  $\text{H}_2$  was introduced into the furnace at a flow rate of 300 ml/min. The synthesis parameters used for CNT growth were then similar to those we have reported previously [20]. Briefly, after 30 min reduction heating at  $780^\circ\text{C}$ , a 40% camphor solution in acetone was injected into the reaction quartz tube at a rate of 0.8 ml/h for 90 min. The furnace was then cooled to room temperature to obtain the composite filter. A schematic of the experimental set up has been shown in supporting information (SI) section S1. Finally the CNT filters were functionalized prior to filtration testing either through oxidisation at  $400^\circ\text{C}$  in air for 2 h, or incubating in preheated nitric acid solution (70%) at ca.  $100^\circ\text{C}$  for 30 min [21].

Scanning electron microscopy (SEM), transmission electron microscopy (TEM) and thermal gravity analysis (TGA) were used to characterise the CNT composite filters. For TEM sample preparation the CNT-ceramic filter was first milled into powder in a mortar, which was then sonicated in acetone before transferring a drop of the suspension onto a carbon copper grid. In addition 3D imaging of the composite filters was performed using an *X-tek BenchTop 160Xi CT* scanning system, in which the sample was X-rayed over 360 degrees to create a 3D model of the filter.

## 2.2 Filtration tests

The CNT composite filters were tested for their ability to remove microorganisms and heavy metal ions from water and particulate filtration of the air. Filter efficiency will be calculated by counting the differences between the amount of contaminant concentrations in the media (air and water) before and after the filtration. For the liquid filtration experiments the composite filter was placed in a vertical quartz tube before injecting yeast or heavy metal ion solutions and the effect of filter length and injection rates were investigated.

To study microorganism removal the model yeast *Saccharomyces cerevisiae*, BY4741 [22], was grown to mid exponential phase in YEPD complete media (1% Yeast extract, 2% Peptone, 2% Glucose). Cells were then harvested by centrifugation and re-suspended in phosphate buffered saline at a concentration of  $1 \times 10^7$  cells/ml, and after filtration the number of cells in the flow through was determined by haemocytometer counts. For heavy metal ion removal the concentration of iron, copper, cobalt, manganese and zinc ions post filtration was determined by inductively coupled plasma mass spectrometry (ICP-MS) using an Agilent 7700x series. Finally for airborne particle filtration a Lighthouse portable airborne laser particle counter (SOLAIR 3100) was used to monitor the concentration of particles ranging from 0.3-10  $\mu\text{m}$  in ambient air passing through the filter.

### 3. Results and discussion

#### 3.1 CNT Filter fabrication process

The physical change in appearance of the ceramic after CNT deposition can be seen in Fig. 1a and 1b, where the densely deposited CNT layers located in the inner wall of the ceramic matrix are clearly evident. A  $\mu\text{CT}$ -scan (Fig. 1c) also shows the interconnectivity of pores across the substrate, demonstrating that uniform catalyst deposition and CNT growth in all sections of the matrix is possible. A range of temperatures from 500 to 900°C was examined, and 780°C was chosen as the optimum temperature where good quality CNTs were deposited on all sections of the ceramic matrix as visualized by SEM analysis (Fig. 1d). The effect of temperature on CNT growth has been described in the SI, section S2. TEM results also clearly revealed that the resulting nanomaterials are hollow, being CNTs rather than solid carbon nanofibres, with an average diameter of 40 nm and lengths of up to several micrometres. Tip growth is the dominating mechanism of CNT growth mechanism, and as expected catalyst particles could be detected at the tip of nanotubes (Fig. 1e). It is difficult to estimate the total CNT contents in a filter; however based on the weight loss recorded

between 530°C and 700°C during TGA analysis we believe the CNT content to be approximately 3%.

Camphor is an environmentally friendly, cheap carbon source which has been successfully used for fabrication of C60 [23] and CNTs [24]. Unlike other reports, which have used a solid source of camphor, a solution of camphor in acetone was used in this work in order to allow a precise and continuous injection rate into the reaction chamber. This is required alongside the uniform distribution and small size of catalyst particles, temperature and H<sub>2</sub> injection rate in ensuring the quality and yield of CNTs. The formation of a viable nucleation site from the catalyst precursor under these conditions has been explained in our previous work [20].

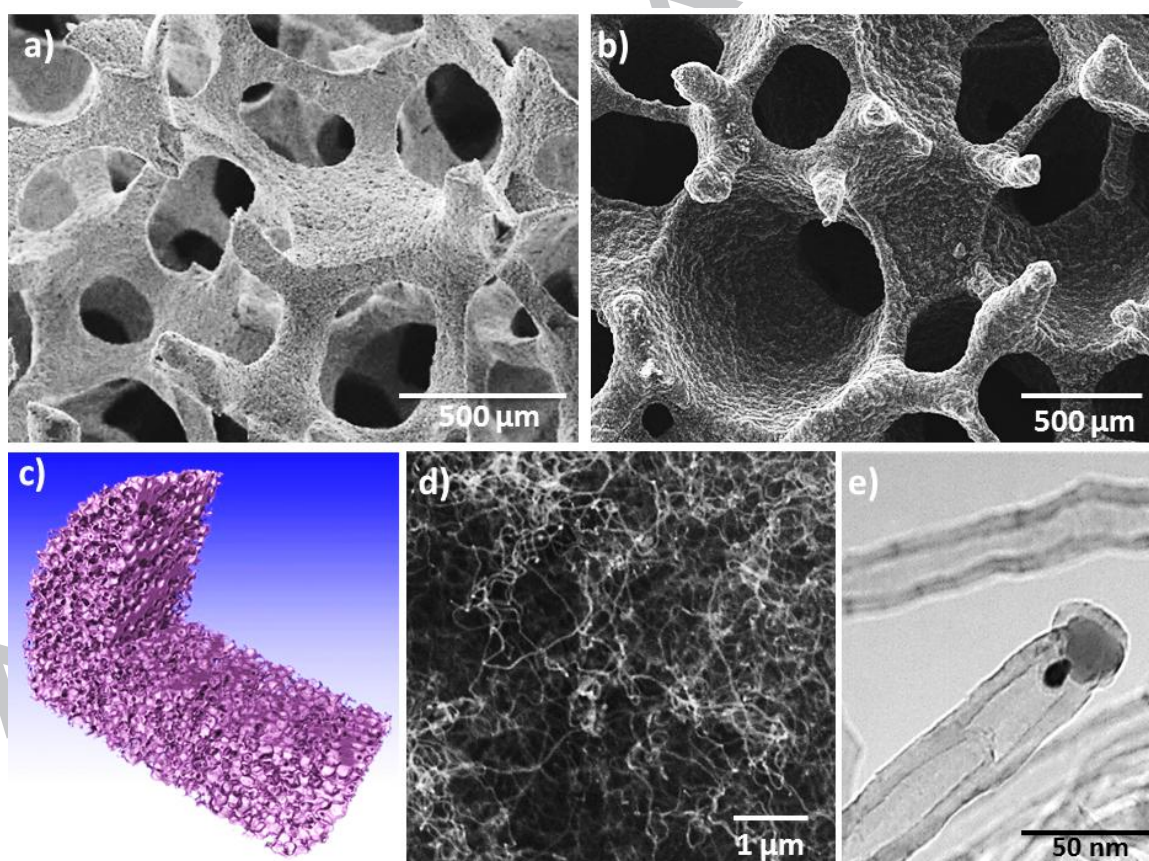


**Fig. 1 - The composite filter and its components.** **a**, Low magnification SEM images of a porous ceramic matrix before CNT growth; **b**, Low magnification SEM image of ceramic/CNT composite after CNT growth; **c**, 3D image of a ceramic substrate following a  $\mu$ -

CT scan showing the interconnectivity of pores; **d**, SEM image exhibiting the high quality and quantity of CNTs grown on the ceramic disc; **e**, TEM image of CNTs collected from the filter. The hollow structural feature of the nanotubes can be clearly seen. A catalyst (dark particle) is visible at the tip.

### 3.2 Yeast filtration

To visualise yeast cells post-filtration the filter was carefully cut open to expose the internal structures, dried at 100°C for several hours and examined by SEM. Due to the high conductivity of CNT, all SEM investigations were performed without any coating. Fig. 2 shows the captured yeast cells (large bright particles) attached to CNT surfaces. At higher magnification it was found that yeast cells were captured by the tangled CNT networks. We believe that this tangled network on the surface of the internal filter cavity can physically ‘capture’ and immobilize the yeast cells whilst allowing water to pass through (Fig. 2d). The pit identified in Fig. 2a is believed to arise from a yeast cell being displayed following the filter being cut open, and the overall size of these pits must have been increased during the drying out process owing to shrinkage of both CNT networks and the cells.



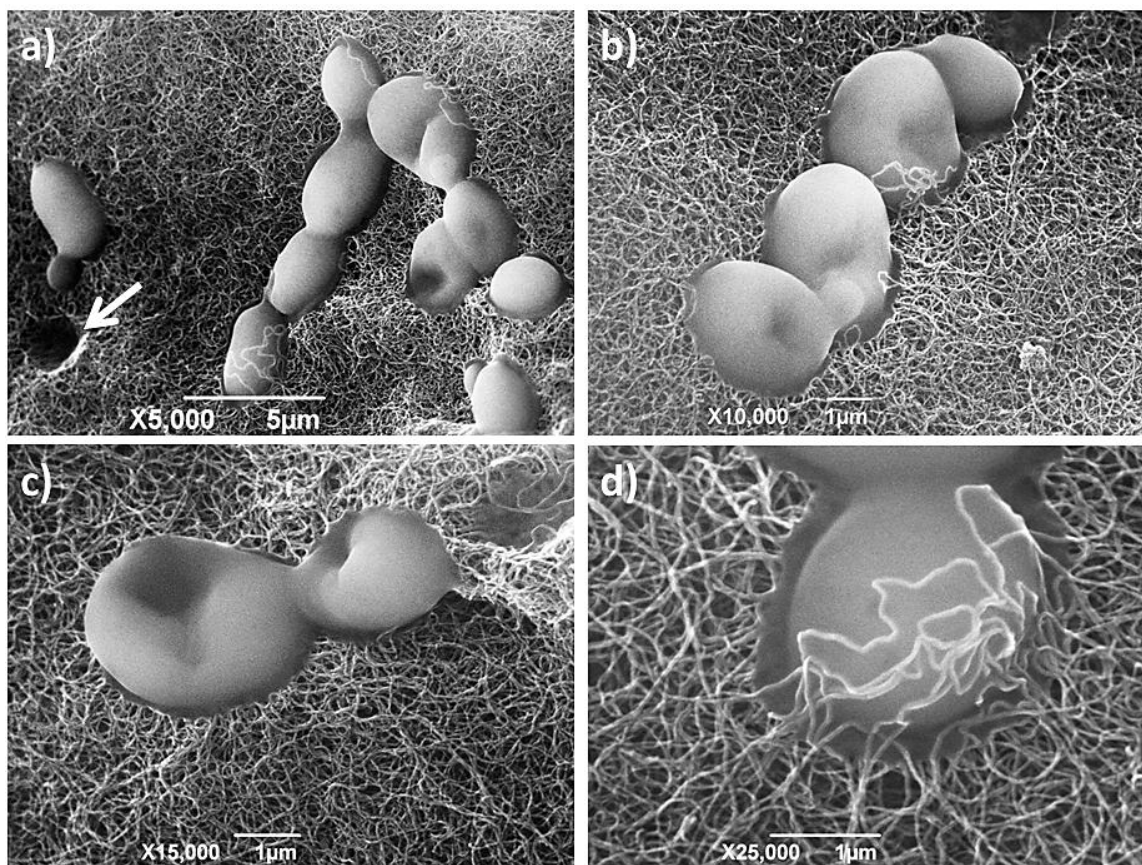


**Fig. 2 - SEM images of the filtered yeast cells by CNTs at different magnifications. The tangled CNTs are closely connected with the yeast cells and have immobilised them.**

Filter length and aqueous flow rate were both shown to have a strong influence on the overall efficiency of yeast filtration, and the results are summarised in Fig. 3. Filter lengths of both 50 and 70 mm reached a maximum efficiency of 98% yeast filtration at a flow rate of 20 ml/h. A reduced flow rate of 10 ml/h was also tested but no further improvement in efficiency was observed. Parallel experiments, using ceramic filters without CNTs were also performed, and a 20 mm long filter at a 20 ml/h flow rate only achieved an filtration efficiency of <5%, possibly due to physical blockage, as opposed to the 68% efficiency obtained using a 20 mm long CNT filter at a similar flow rate. These results clearly demonstrate that CNTs play the decisive role in the filter, and that efficiency is increased with a lower liquid flow rate and longer filters. A lower liquid flow rate would presumably allow a longer interaction time

between the CNT network and the yeast cells, whilst longer filters would offer more barriers to the cells to result in improved efficiency.

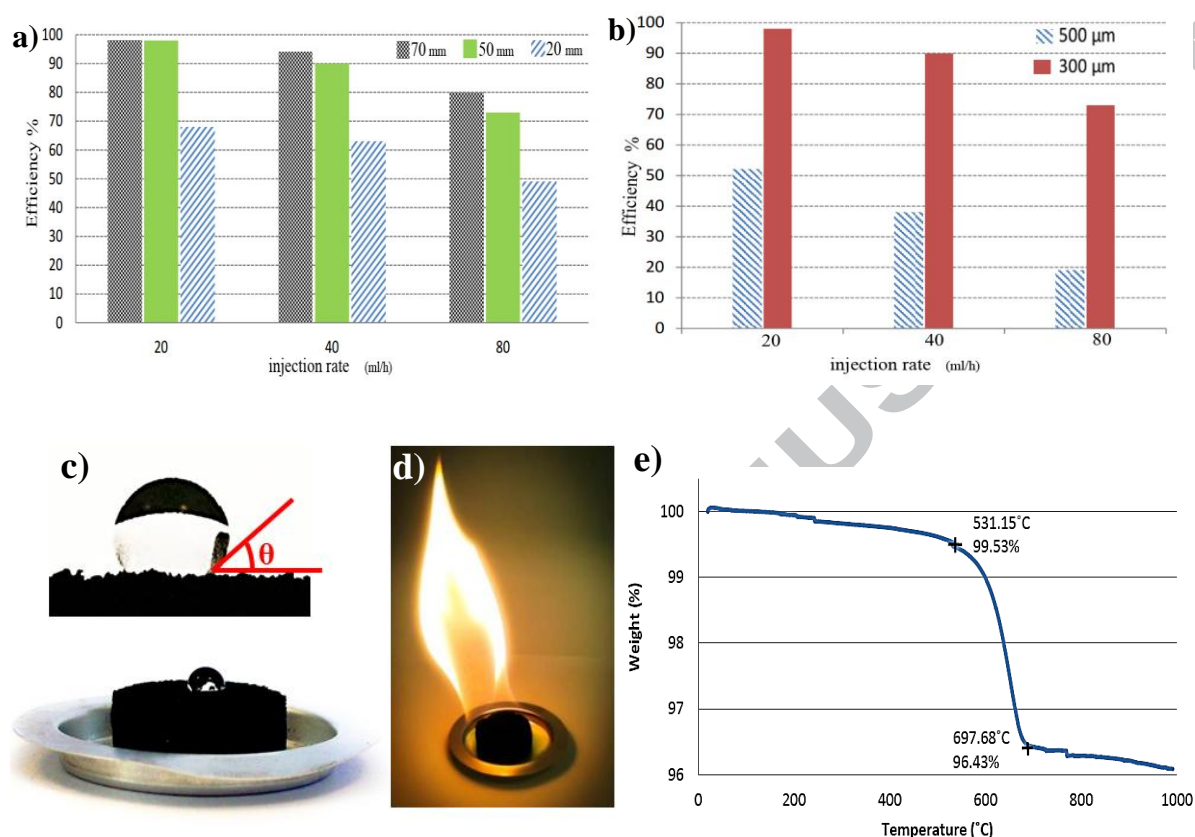


**Fig. 3 - Composite filter efficiency for yeast cells and the role of CNTs in the filtration.** **a**, Composite filter efficiency for yeast as a function of filter length and injection rate; **b**, Composite filter efficiency for yeast as a function of filter length and pore sizes; **c**, An illustration of the surface hydrophobic behaviour of filter with as-grown CNTs; **d**, A disc filter burning after filtration of yeast cells by adding acetone, showing a possible route for the filter regeneration; and **e**, TGA result indicating high thermal stability of CNTs and confirming the success of the filter regeneration.

To determine the influence of initial pore size we conducted experiments using 50 mm CNT filters prepared from ceramics displaying either 300 or 500  $\mu\text{m}$  pores (Fig. 3b). Higher efficiencies of filtration for CNT filters with a 300  $\mu\text{m}$  pore size, across a range of flow rates,

are obvious compared to that of the 500  $\mu\text{m}$  filter. Therefore the use of a finer pore sized matrix clearly helps to achieve higher efficiency. However, the use of filters with even finer pore sizes would pose a challenge for ensuring uniform CNT growth inside the pores. Previously, we have reported the successful production of CNTs in bulk ceramics with a pore size of between 100-150  $\mu\text{m}$  [20]. However, when using filters with finer pore sizes, it would be extremely difficult to produce CNTs uniformly in centimetre scale samples. Fig. 3c exhibits the hydrophobic behaviour of the CNT filters which originates from the hydrophobic characteristics of the prepared CNTs [25].

Compared to membranes that are used for micro and nanofiltration the current composite filters have obvious advantages, such as being robust and durable and in particular their reusability. Due to the high thermal stability and resistance of both the matrix and CNTs the bio-contaminants inside the filter can simply be burnt off (Fig. 3d) to recycle the filter without damaging the CNTs. TGA analysis of the remaining CNTs after burning (Fig. S3) demonstrated an identical pattern of weight loss at temperatures over 530°C to pristine unused CNT filters, proving the undamaged profile of CNTs in the filter. Visualisation of the filter through SEM and TEM analysis also led to the same conclusion (Fig. S3). Furthermore, we verified that the recycled filters resulted in negligible differences in filtration efficiency (Fig. S4). Therefore, these CNT/ceramic composites display promising robust and reusable features.

### 3.3 Air particulate filtration

Air filters for heating, ventilation and air conditioning (HVAC) typically work in the dark and damp and at ambient temperatures therefore providing ideal conditions for microbial growth. The situation becomes worse when micro-organisms adhere to accumulated dust on the filter and proliferate, resulting in an unpredictable deterioration of air quality and the production of bad odours [26]. This issue may be circumvented through the use of CNTs as

these display inherent antibacterial properties in addition to their potentially improved mechanical properties and filtration efficiency. Fig. 4 displays the filtration efficiencies of air particulates for 300 and 500  $\mu\text{m}$  pore sized filters with and without CNTs. The results clearly show that the incorporation of CNTs dramatically increases the filtration efficiencies of these filters compared to plain ceramics, and in particular for the smaller particle sizes of 0.3 and 0.5  $\mu\text{m}$ . For example a 100 mm long composite filter can stop 90% and 95% of 0.3 and 0.5  $\mu\text{m}$  particles respectively compared with an efficiency of just 28% and 60% for plain ceramic filters. This improvement can be explained by considering the Brownian diffusion mechanism, where longer filters result in a decreased velocity of gas flow allowing particles to have more time to interact with the CNTs on the pore surface, and a nose hair effect is believed to be the main mechanism for blocking these particulates. In this regard, and consistent with the results reported by Guan and Yao [27], the loading of CNTs is the dominating factor on filtration efficiency compared to ceramic pore size. The initial efficiency of 0.5  $\mu\text{m}$  particulate filtration for a the 300  $\mu\text{m}$  pore sized plain ceramic is higher than that of a CNT-500  $\mu\text{m}$  pore sized filter for a short 10 mm filter (Fig. 4b), but increasing the filter length, to increase exposure to CNTs, gradually raised the filtration efficiencies. For example for the 100 mm long filter the CNT-500  $\mu\text{m}$  filter reached 85% efficiency compared to 60% for the 300  $\mu\text{m}$  pore sized plain ceramic filter. Interestingly, a 10 mm long CNT-300  $\mu\text{m}$  filter or a 20 mm long CNT-500  $\mu\text{m}$  filter is sufficient to capture all particles  $\geq 5 \mu\text{m}$ , which is equivalent to a 80 mm or 100 mm long filter with a pore size of 300  $\mu\text{m}$  or 500  $\mu\text{m}$  respectively. For such big particles, inertia impaction and interception accounts for the filtration mechanism [28].

Fig. 4c summarises the efficiencies of longer filters for particles sized less than 5  $\mu\text{m}$ . It can be seen that for a 300 mm long composite filter it is possible to capture more than 99.6% of particles ( $> 0.3 \mu\text{m}$ ) in air. It is noted that after reaching 90% efficiency, further

improving of the efficiency to almost 100% requires much more effort. For example increasing the filter length from just 10 to 20 mm for the CNT-300  $\mu\text{m}$  filter almost doubles the efficiency (Fig. 4a), but an increase in filter length from 200 to 300 mm leads to only a 1.2% increase in efficiency (Fig. 4c). It is also noteworthy that the pristine CNT filters and air-oxidized CNT filters exhibited very similar efficiencies for particulate filtration in air, which suggests that the mechanism of filtration is mainly through physical interception (Detailed information is provided in the SI section S4).

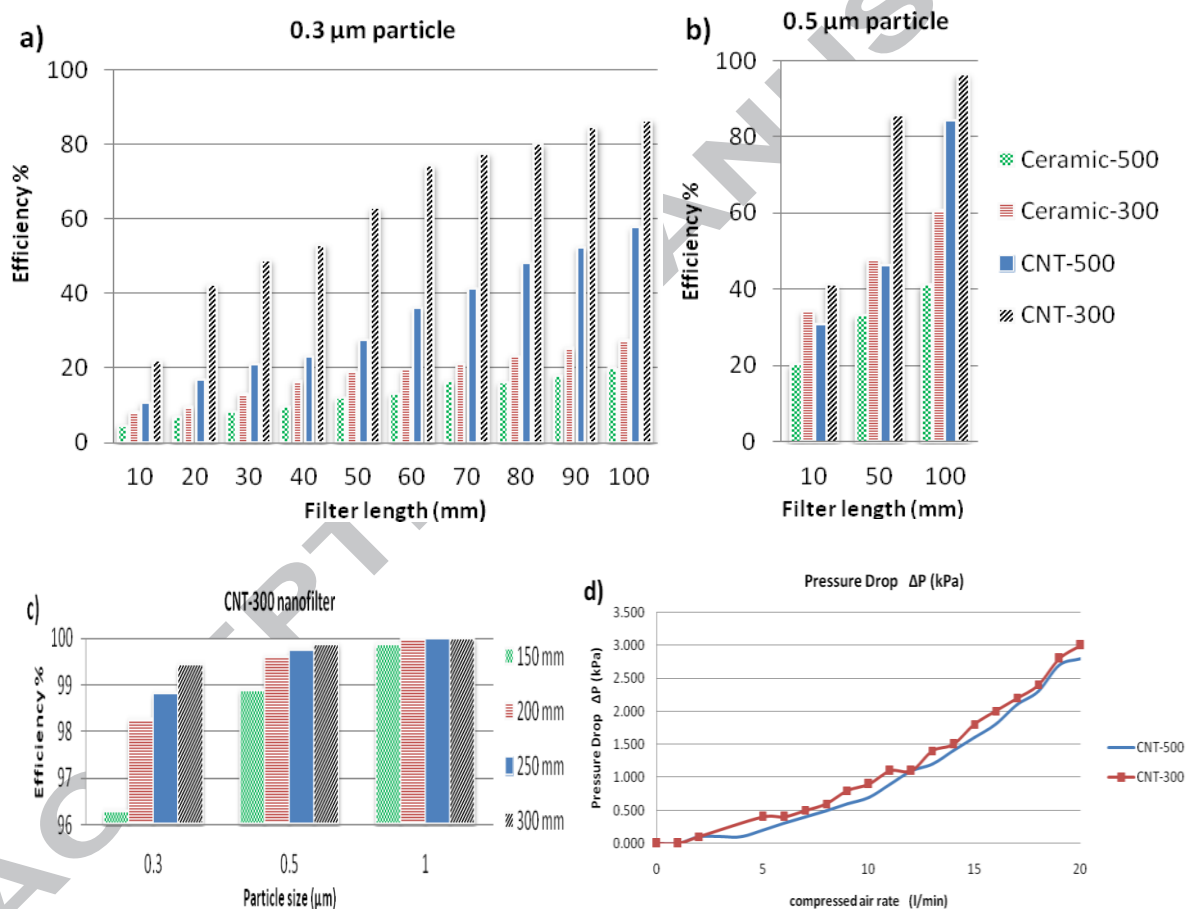


**Fig. 4 - The effect of different parameters on air particulate filtration efficiency. a,** Air particulate filter efficiency as a function of filter length for 0.3  $\mu\text{m}$  particles. **b,** Air particulate filter efficiency as a function of filter length for 0.5  $\mu\text{m}$  particles. **c,** Filtration efficiency as a

function of particle size. **d**, Pressure drop of a 10 mm ceramic filter as a function of the air flow rate.

Pressure drop is an important factor in gas filtration. As shown in the  $\mu$ -CT scan image in Fig. 1c, the ceramic substrate consists of randomly interconnected channels laid in different directions which would increase the pressure drop associated with using these filters. However, the thin coating of CNT on the ceramic matrix has a negligible effect on the pressure drop seen with these current filters. The pressure drop caused by these filters suggests that these filters may suit air filtration applications where the air flow rate is low or pressure drop is not essential. However, for situations where pressure is more critical, it would be possible to modify the substrate pore or channel configuration using a specifically designed unidirectional ceramic template. By then applying the same CNT composite filter fabrication method it should be possible to make highly stable and efficient particulate filters with a lower pressure drop, suitable for applications such as diesel particulate filters for engines.

### 3.4 Metal ion removal

Prior to investigating the CNT composite filter in the removal of heavy metal ions from water, the plain porous ceramics were tested in order to rule out their effect. A negligible adsorption capacity of less than 4% was recorded with the ceramic filters, therefore, any higher binding efficiency can be attributed to the presence of CNTs.

As it was shown in Fig. 3c, the CNT filters exhibit hydrophobic behaviour. Thus, functionalization of the CNTs to modify their surface behaviour is therefore an important step for the filter to be utilized in aquatic systems, where improved wettability is desirable for many practical applications [4]. It is possible to modify the sidewalls or ends of CNTs with either covalent or non-covalent attachments in order to achieve better surface contact with the

adsorbents. However, this type of surface treatment typically involves chemical treatments which lead to localized CNT densification and bundle formation on the ceramic surfaces during the drying process. Such changes can reduce the effective contact area of the filter resulting in a reduced functionality for some applications. Therefore we also employed an alternative air oxidation process (at 400 °C) to modify the CNTs in the filter as, compared with the wet chemistry method, this allows the maintenance of the original orientation and distribution of CNTs in the filter.

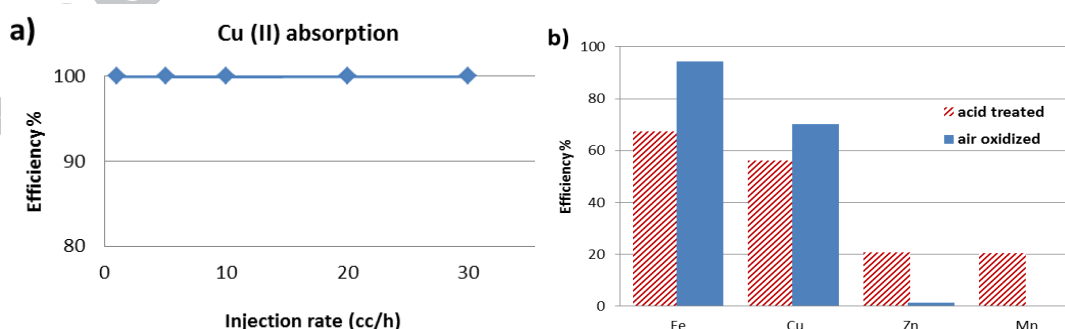
As presented in Fig. 5a the initial adsorption efficiency of an air oxidized 20 mm long CNT filter for  $\text{Cu}^{2+}$  ions (from 12 mg/ml  $\text{CuCl}_2$ ) reached  $99.99\% \pm 0.01$  in solution flow rates from 2 to 30 ml/h. This would suggest that almost all  $\text{Cu}^{2+}$  ions can be removed regardless of flow rates of the solution. Whilst this is extremely promising in reality most instances of water contamination contain multiple heavy metal ions. Therefore a systematic investigation was carried out to explore the ability of our composite filters to adsorb a mixture of metal ions. It is to be expected that the different surface functional groups, introduced during the functionalization of CNTs/ceramic composite via either acid treatment or air oxidation at 400 °C, would have a strong influence on metal ion adsorption. Initially 10 mm long functionalized CNT filters were immersed in a 30 ml solution of  $\text{Fe}^{2+}$ ,  $\text{Cu}^{2+}$ ,  $\text{Zn}^{2+}$  and  $\text{Mn}^{2+}$  ions (each at a concentration of 5 mg/l) for 10 h to reach a binding equilibrium. As shown in Fig. 5b the air oxidized filter adsorbed most of the  $\text{Fe}^{2+}$  and  $\text{Cu}^{2+}$  ions, with only a negligible amount of adsorption for  $\text{Zn}^{2+}$  and  $\text{Mn}^{2+}$ . In contrast the acid functionalised filter adsorbed ~20%  $\text{Zn}^{2+}$  and  $\text{Mn}^{2+}$  ions under the same conditions. However, interestingly the sum total of heavy metal ions absorbed was almost identical between filters at 40% (Fig. S6). This result has demonstrated that in the presence of mixed ions their competitive binding to CNTs dominates the adsorption process. Air oxidization and acid functionalization of CNT filters can introduce oxygen-containing functional groups into the CNT surface, which make the

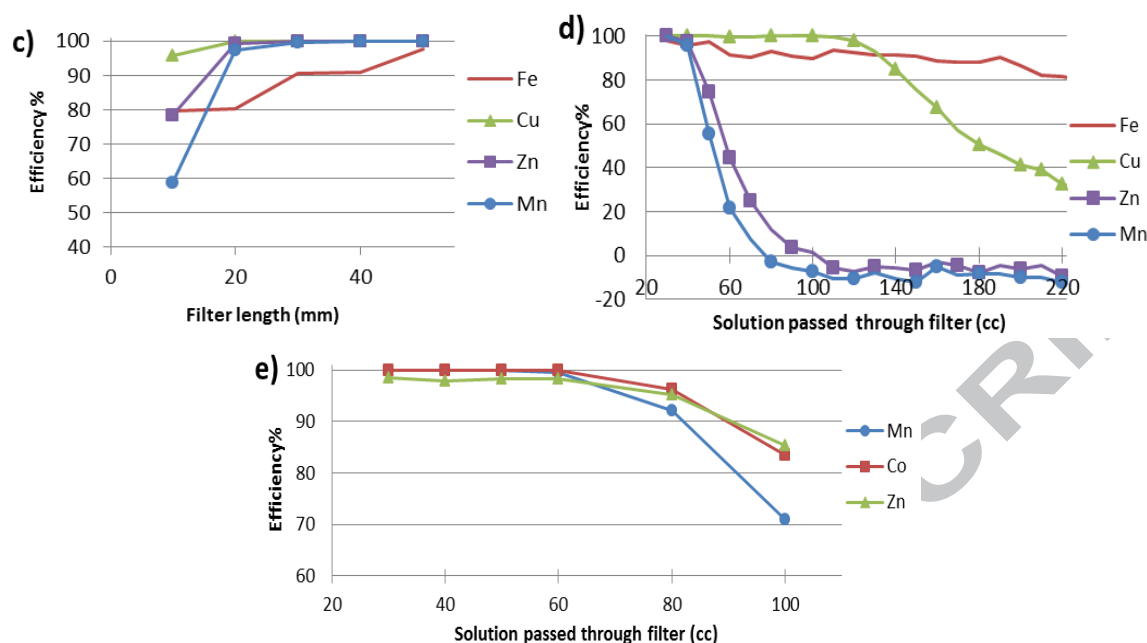
filters be hydrophilic that can form strong interaction with metal ions of high electronegativity. In the mixed metal ions solution, both  $\text{Fe}^{2+}$  and  $\text{Cu}^{2+}$  have higher electronegativity (1.83 and 1.90 respectively) than the other two metals  $\text{Zn}^{2+}$  and  $\text{Mn}^{2+}$  (1.65 and 1.55 respectively). As a consequence of competitive adsorption,  $\text{Fe}^{2+}$  and  $\text{Cu}^{2+}$  can be preferably adsorbed by the hydrophilic CNT surfaces, leaving  $\text{Zn}^{2+}$  and  $\text{Mn}^{2+}$  ions with low or almost no adsorption. This experiment has also demonstrated that the acid functionalized CNTs provided more active groups for  $\text{Zn}^{2+}$  and  $\text{Mn}^{2+}$  ion binding than that of the air oxidised filter. The adsorption capacity of CNTs for metal ions strongly depends upon their surface acidity, increasing with a rise in the number of acid groups (including carboxyl, lactones and phenols) [19]. The chemical and thermal treatments used during functionalization can affect the nature and concentration of the surface functional groups displayed. Note that however, it is also likely that the presence of fulvic acids during the nitric acid functionalization of the filter could result in additional oxygen groups on the CNT surface, which also contributed to the adsorption process [29-31]. Base wash is an effective approach for completely neutralizing this effect which has not been considered in present work. The surface of untreated CNTs is known to contain a small amount of basic functional groups, in addition to amorphous carbon, carbon black and carbon particles. Gas phase oxidation at  $400^\circ\text{C}$  can introduce hydroxyl and carbonyl functional surface groups. Liquid acid oxidation can also generate carboxylic acid functional groups on the surface of CNTs, and in addition remove amorphous carbon from the CNT surfaces. These changes can facilitate the ion-exchange capability of CNTs, as the introduced functional groups cause a rise in negative charge on the carbon surface and the oxygen atoms in functional groups can donate electrons resulting in a higher cation exchange capacity [3, 13].

Fig. 5c shows the filtration efficiencies versus filter length for the removal of  $\text{Fe}^{2+}$ ,  $\text{Mn}^{2+}$ ,  $\text{Zn}^{2+}$  and  $\text{Cu}^{2+}$  ions for acid treated filters at an injection rate of 120 ml/h.  $Q_e$  (equilibrium



uptake, mg/g) versus  $C_e$  (heavy metal ions concentration, mg/l) graph would normally be used to represent the maximum uptake value and the adsorption isotherm profile. However, this requires precise quantifying the exact amount of CNTs on each filter, which is challenging at the time. Using estimations by weighting the filters after and before the CNT growth would give a noteworthy error due to the involvement of both Ni catalyst and CNTs. Furthermore challenge is to obtain filters with different CNT concentrations for producing the  $Q_e/C_e$  graph, which is an ongoing investigation. As expected longer filters, containing more CNTs, resulted in a higher adsorption efficiency, reaching approximately 100% efficiency with a 50 mm filter independent of the injection rate. We also tested the effect of saturation of the filter, through the continual passage of the solution, in order to determine its relative affinities for the different metal ions. After passing through over 40 ml of solution, the amount of  $Mn^{2+}$  and  $Zn^{2+}$  ions adsorbed quickly dropped to 0%, whilst the binding of  $Fe^{2+}$  and  $Cu^{2+}$  ions remained relatively high and stable. Indeed it appears that when more solution is passed through the filter releases the adsorbed  $Mn^{2+}$  and  $Zn^{2+}$  ions back into the solution indicating they are completely lost in competition with  $Cu^{2+}$  and  $Fe^{2+}$ . Furthermore as even more solution is passed through the filter  $Fe^{2+}$  ions ultimately out compete  $Cu^{2+}$  ions for binding sites and  $Cu^{2+}$  ions are released.





**Fig. 5 - Filtration efficiency of functionalised CNTs/ceramic for heavy metal ions. a,** single  $\text{Cu}^{2+}$  adsorption as a function of injection rate using 20 mm long filters. **b,** Adsorption efficiency of 10 mm long functionalized filters for 30 ml of heavy metal solution containing 5 mg/l of each of  $\text{Fe}^{2+}$ ,  $\text{Cu}^{2+}$ ,  $\text{Mn}^{2+}$  &  $\text{Zn}^{2+}$  ions. One filter was oxidized in air and the other treated in acid. **c,** Adsorption efficiency of filters as a function of their length using the same solution as in (b). **d,** Saturation point of a 50 mm long filter using the same solution as in (b). **e,** Saturation point of a 50 mm long filter using heavy metal ion solutions containing 5 mg/l of each of  $\text{Co}^{2+}$ ,  $\text{Mn}^{2+}$  &  $\text{Zn}^{2+}$ .

As  $\text{Fe}^{2+}$  and  $\text{Cu}^{2+}$  ions have much higher adsorption tendencies compared to  $\text{Mn}^{2+}$  and  $\text{Zn}^{2+}$ , they were replaced with  $\text{Co}^{2+}$  ions in order to investigate the adsorption efficiency of these heavy metals ions in a less competitive condition (Fig. 5e). In this case the filter exhibited similar efficiencies for all three ions with over 95% of ions retained when up to 80 ml of solution was passed through the filter, indicating a much higher saturation point in a less competitive environment.

Injection rates from 1 - 500 ml/h were also tested, and only a 15% drop in adsorption efficiency was observed when changing the solution flow rate from 120 ml/h to 500 ml/h using the 20 mm filter and a 5 mg/l solution of heavy metal ions ( $\text{Co}^{2+}$ ,  $\text{Mn}^{2+}$  and  $\text{Zn}^{2+}$ ; Fig. S7). This would suggest that the current filter could be used in a faster stream whilst maintaining high efficiency (SI section S6). It would also be possible to have the same complete ion removal at higher injection rates by increasing the length of filter, alternatively increasing the temperature may also improve adsorption efficiency as was previously shown by Lu et al. [32] for  $\text{Zn}^{2+}$ .

In order to justify the high initial cost of CNT filters and introduce them as a practical solution for challenges in wastewater treatment, it is also important to know the reusability of the composite filters. It has been well-discussed in the literature that it is possible to desorb metal ions from CNTs in acidic solutions ( $\text{pH} < 2$ ) without a noticeable drop in their subsequent filtration efficiency [19], and we were also able to reuse our filters several times by desorbing the metal ions in an acidic solution ( $\text{HNO}_3$ ). However, it has also been evidenced that during the acidic desorption process small amounts of CNTs are released into the solution. As the toxicity of CNTs themselves is a concern [33] it is important to take this fact into account and a possible secondary protective process to capture the potentially released CNTs, such as placing a membrane in the outlet of filters, should be employed. Finally, compared with most recent reports where loose CNT powders were soaked in solutions for several hours before their collection through filtering [3, 18, 32], which time consuming and less controllable, the current composite filters are robust, cheap, highly efficient, versatile and reusable. As such we hope that these results will be an important step towards the application of CNT filters at an industrial scale.

#### 4. Summary

Experimental assessment of CNT/ceramic composite filters fabricated by one step direct growth using CVD have confirmed that they can be used in a wide range of applications for the removal of micro-organisms and heavy metal ions from water and airborne particulates in air, with very high efficiencies. Further development of the robust, cheap, reusable and versatile filters may find successful nanotechnology applications in industries where filtration is required.

### **Acknowledgment**

Thank EPSRC for financial support. Thank Dr L Wears for help with experiments.

## References

- [1] Mitsakou C, Housiadas C, Eleftheriadis K, Vratolis S, Helmis C, Asimakopoulos D. Lung deposition of fine and ultrafine particles outdoors and indoors during a cooking event and a no activity period. *Indoor Air*. 2007;17(2):143-52.
- [2] Hillie T, Hlophe M. Nanotechnology and the challenge of clean water. *Nat Nano*. 2007;2(11):663-4.
- [3] Li YH, Ding J, Luan Z, Di Z, Zhu Y, Xu C, et al. Competitive adsorption of Pb<sup>2+</sup>, Cu<sup>2+</sup> and Cd<sup>2+</sup> ions from aqueous solutions by multiwalled carbon nanotubes. *Carbon*. 2003;41(14):2787-92.
- [4] Upadhyayula VKK, Deng S, Mitchell MC, Smith GB. Application of carbon nanotube technology for removal of contaminants in drinking water: A review. *Science of The Total Environment*. 2009;408(1):1-13.
- [5] Barkauskas J. pH-dependent water penetration through CNT sub-layers arranged on the polycarbonate membrane filters. *Carbon*. 2010;48(6):1858-61.
- [6] Smajda R, Kukovec Á, Kónya Z, Kiricsi I. Structure and gas permeability of multi-wall carbon nanotube buckypapers. *Carbon*. 2007;45(6):1176-84.
- [7] Halonen N, Rautio A, Leino AR, Kyllonen T, Toth G, Lappalainen J, et al. Three-Dimensional Carbon Nanotube Scaffolds as Particulate Filters and Catalyst Support Membranes. *ACS Nano*. 2010;4(4):2003-8.
- [8] Park SJ, Lee DG. Performance improvement of micron-sized fibrous metal filters by direct growth of carbon nanotubes. *Carbon*. 2006;44(10):1930-5.
- [9] Park JH, Yoon KY, Na H, Kim YS, Hwang J, Kim J, et al. Fabrication of a multi-walled carbon nanotube-deposited glass fiber air filter for the enhancement of nano and submicron aerosol particle filtration and additional antibacterial efficacy. *Science of The Total Environment*. 2011;409(19):4132-8.
- [10] Srivastava A, Srivastava ON, Talapatra S, Vajtai R, Ajayan PM. Carbon nanotube filters. *Nat Mater*. 2004;3(9):610-4.
- [11] Brady-Estevez AS, Kang S, Elimelech M. A Single-Walled-Carbon-Nanotube Filter for Removal of Viral and Bacterial Pathogens. *small*. 2008;4(4):481-4.
- [12] Brady-Estévez AS, Nguyen TH, Gutierrez L, Elimelech M. Impact of solution chemistry on viral removal by a single-walled carbon nanotube filter. *Water Research*. 2010;44(13):3773-80.
- [13] Stafiej A, Pyrzynska K. Adsorption of heavy metal ions with carbon nanotubes. *Separation and Purification Technology*. 2007;58(1):49-52.
- [14] Lu C, Liu C. Removal of nickel(II) from aqueous solution by carbon nanotubes. *Journal of Chemical Technology and Biotechnology*. 2006;81(12):1932-40.
- [15] Di ZC, Ding J, Peng XJ, Li YH, Luan ZK, Liang J. Chromium adsorption by aligned carbon nanotubes supported ceria nanoparticles. *Chemosphere*. 2006;62(5):861-5.
- [16] Luo G, Yao H, Xu M, Cui X, Chen W, Gupta R, et al. Carbon Nanotube-Silver Composite for Mercury Capture and Analysis. *Energy & Fuels*. 2009;24(1):419-26.
- [17] Schierz A, Zänker H. Aqueous suspensions of carbon nanotubes: Surface oxidation, colloidal stability and uranium sorption. *Environmental Pollution*. 2009;157(4):1088-94.
- [18] Tofighy MA, Mohammadi T. Adsorption of divalent heavy metal ions from water using carbon nanotube sheets. *Journal of Hazardous Materials*. 2011;185(1):140-7.
- [19] Rao GP, Lu C, Su F. Sorption of divalent metal ions from aqueous solution by carbon nanotubes: A review. *Separation and Purification Technology*. 2007;58(1):224-31.
- [20] Parham H, Kennedy A, Zhu Y. Preparation of porous alumina-carbon nanotube composites via direct growth of carbon nanotubes. *Composites Science and Technology*. 2011;71(15):1739-45.

- [21] Li YH, Di Z, Ding J, Wu D, Luan Z, Zhu Y. Adsorption thermodynamic, kinetic and desorption studies of Pb<sup>2+</sup> on carbon nanotubes. *Water Research*. 2005;39(4):605-9.
- [22] Baker Brachmann C, Davies A, Cost GJ, Caputo E, Li J, Hieter P, et al. Designer deletion strains derived from *Saccharomyces cerevisiae* S288C: A useful set of strains and plasmids for PCR-mediated gene disruption and other applications. *Yeast*. 1998;14(2):115-32.
- [23] Mukhopadhyay K, Krishna KM, Sharon M. Fullerenes from camphor: A natural source. *Physical Review Letters*. 1994;72(20):3182.
- [24] Kumar M, Ando Y. A simple method of producing aligned carbon nanotubes from an unconventional precursor - Camphor. *Chemical Physics Letters*. 2003;374(5-6):521-6.
- [25] Kanyo T, Konya Z, Kukovec A, Berger F, Dekany I, Kiricsi I. Quantitative Characterization of Hydrophilic-Hydrophobic Properties of MWNTs Surfaces. *Langmuir*. 2004;20(5):1656-61.
- [26] Barhate RS, Ramakrishna S. Nanofibrous filtering media: Filtration problems and solutions from tiny materials. *Journal of Membrane Science*. 2007;296(1-2):1-8.
- [27] Guan T, Yao M. Use of carbon nanotube filter in removing bioaerosols. *Journal of Aerosol Science*. 2010;41(6):611-20.
- [28] Hinds WC. *Aerosol technology : properties, behavior, and measurement of airborne particles*. New York [u.a.]: Wiley; 1999.
- [29] Wang Z, Shirley MD, Meikle ST, Whitby RLD, Mikhalovsky SV. The surface acidity of acid oxidised multi-walled carbon nanotubes and the influence of in-situ generated fulvic acids on their stability in aqueous dispersions. *Carbon*. 2009;47(1):73-9.
- [30] Verdejo R, Lamoriniere S, Cottam B, Bismarck A, Shaffer M. Removal of oxidation debris from multi-walled carbon nanotubes. *Chem Commun (Camb)*. 2007;5:513-5.
- [31] Salzmann CG, Llewellyn SA, Tobias G, Ward MAH, Huh Y, Green MLH. The Role of Carboxylated Carbonaceous Fragments in the Functionalization and Spectroscopy of a Single-Walled Carbon-Nanotube Material. *Advanced Materials*. 2007;19(6):883-7.
- [32] Lu C, Chiu H, Liu C. Removal of Zinc(II) from Aqueous Solution by Purified Carbon Nanotubes: Kinetics and Equilibrium Studies. *Industrial & Engineering Chemistry Research*. 2006;45(8):2850-5.
- [33] Lam CW, James JT, McCluskey R, Hunter RL. Pulmonary Toxicity of Single-Wall Carbon Nanotubes in Mice 7 and 90 Days After Intratracheal Instillation. *Toxicological Sciences*. 2004;77(1):126-34.